

C-band wavelength-swept single-longitudinal-mode erbium-doped fiber ring laser

Kang Zhang* and Jin U. Kang

Department of Electrical and Computer Engineering, The Johns Hopkins University,
3400 N. Charles St., Baltimore, MD 21218, USA

*Corresponding author: kzhang8@jhu.edu

Abstract: A wavelength-swept single-longitudinal-mode erbium-doped fiber ring laser capable of operating at sweeping frequency in the order of a few kHz is designed and demonstrated by using a fiber Fabry-Perot tunable filter and a Sagnac loop incorporated with a 3.5-meter unpumped erbium-doped fiber. The laser operates in continuous-wave (CW) mode and can sweep approximately 45 nm over the entire C-band (1520nm-1570nm) window with linewidth less than 0.7 kHz. The optimum wavelength sweeping frequency in order to achieve the best output power stability was found to be ~20Hz with sweeping-induced power fluctuation of only 0.1%.

©2008 Optical Society of America

OCIS codes: (060.3510) Lasers, fiber; (140.3570) Lasers, single-mode.

References and links

1. C. S. Kim, F. N. Farokhrooz, and J. U. Kang, "Electro-optic wavelength-tunable fiber ring laser based on cascaded composite Sagnac loop filters," *Opt. Lett.* **29**, 1677-1679 (2004).
2. N. Libatique, L. Wang, and R. Jain, "Single-longitudinal-mode tunable WDM-channel-selectable fiber laser," *Opt. Express* **10**, 1503-1507 (2002), <http://www.opticsexpress.org/abstract.cfm?uri=OE-10-25-1503>.
3. M. Choma, M. Sarunic, C. Yang, and J. Izatt, "Sensitivity advantage of swept source and Fourier domain optical coherence tomography," *Opt. Express* **11**, 2183-2189 (2003), <http://www.opticsexpress.org/abstract.cfm?URI=OPEX-11-18-2183>.
4. Y. W. Song, S. A. Havstad, D. Starodubov, Y. Xie, A. E. and W. J. Feinberg, "40-nm-wide tunable fiber ring laser with single-mode operation using a highly stretchable FBG," *IEEE Photon. Technol. Lett.* **13**, 1167-1169 (2001).
5. H. Chen, F. Babin, M. Leblanc, and G. W. Schinn, "Widely tunable single-frequency Erbium-doped fiber lasers," *IEEE Photon. Technol. Lett.* **15**, 185-187 (2003).
6. C. H. Yeh, T. T. Huang, H. C. Chien, C. H. Ko, and S. Chi, "Tunable S-band erbium-doped triple-ring laser with single-longitudinal-mode operation," *Opt. Express* **15**, 382-386 (2007), <http://www.opticsexpress.org/abstract.cfm?uri=oe-15-2-382>.
7. X. P. Cheng, P. Shum, C. H. Tse, J. L. Zhou, M. Tang, W. C. Tan, R. F. Wu, and J. Zhang, "Single-longitudinal-mode erbium-doped fiber laser based on high finesse fiber Bragg grating Fabry-Perot Etalon," *IEEE Photon. Technol. Lett.* **20**, 976-978 (2008).
8. B. Fischer, J. L. Zyskind, J. W. Sulhoff, and D. J. DiGiovanni, "Nonlinear wave mixing and induced gratings in erbium-doped fiber amplifiers," *Opt. Lett.* **18**, 2108-2110 (1993).
9. S. J. Frisken, "Transient Bragg reflection gratings in erbium-doped fiber amplifiers," *Opt. Lett.* **17**, 1776-1778 (1992).
10. J. Liu, J. P. Yao, J. Yao, and T. H. Yeap, "Single-longitudinal-mode multiwavelength fiber ring laser," *IEEE Photon. Technol. Lett.* **16**, 1020-1022 (2004).
11. A. Yariv, *Optical electronics in modern communications* (Oxford University Press, 1997).
12. S. Fleming and T. Whitley, "Measurement and analysis of pump dependent refractive index and dispersion effects in erbium-doped fiber amplifiers," *IEEE J. Quantum Electron.* **32**, 1113-1121 (1996).
13. E. Desurvire, *Erbium-doped fiber amplifiers: Principles and Applications* (John Wiley & Sons, 1994).
14. X. W. Shu, S. Jiang, and D. Huang, "Fiber Grating Sagnac Loop and Its Multiwavelength-Laser Application," *IEEE Photon. Technol. Lett.* **20**, 980-982 (2000).
15. A. Othonos and K. Kalli, *Fiber Bragg gratings: Fundamentals and Applications in Telecommunications and sensing* (Artech House, 1999).

16. R. N. Liu, I. A. Kostko, R. Kashyap, K. Wu, and P. Kiiveri, "Inband-pumped, broadband bleaching of absorption and refractive index changes in erbium-doped fiber," *Opt. Commun.* **255**, 65-71 (2005).
17. D. Chen, C. Shu, and S. He, "Multiple fiber Bragg grating interrogation based on a spectrum-limited Fourier domain mode-locking fiber laser," *Opt. Lett.* **33**, 1395-1397 (2008).
18. S. H. Yun, G. J. Tearney, J. F. de Boer, N. Iftimia, and B. E. Bouma, "High-speed optical frequency-domain imaging," *Opt. Express* **11**, 2953-2963 (2003), <http://www.opticsinfobase.org/abstract.cfm?URI=oe-11-22-2953>

1. Introduction

Tunable and wavelength-swept single-longitudinal-mode (SLM) lasers have many important applications such as high-resolution spectroscopy, gas sensors, WDM optical communication technology, and swept source Fourier domain optical coherent tomography [1-3]. Tunable SLM erbium-doped fiber (EDF) ring lasers are good candidates for those applications due to their broad tuning range, high output power, and narrow linewidth [4,5]. However, EDF ring lasers usually suffer from multimode oscillation, mode hopping and competing due to their long cavity length and thus narrow longitudinal mode spacing. Therefore narrow-bandwidth mode selecting mechanism is required to ensure SLM operation, and the mode selecting mechanism should also be wavelength-tunable over a wide spectral range. Various schemes have been demonstrated to show both SLM and tunability simultaneously, for example, using such schemes as a multi-ring cavity with a band pass filter [6], a tunable fiber Bragg grating (FBG) Fabry-Perot etalon [7], and a saturable absorber with a tunable FBG [4]. It has been shown in prior works that a section of unpumped EDF in a Sagnac loop can be used as a saturable absorber in which two counter-propagating waves form a standing wave and induce spatial-hole-burning (SHB). The refraction index of the unpumped EDF changes spatially due to SHB and this results in an ultra-narrow bandwidth self-induced FBG [8,9].

In this work, a Sagnac loop with a 3.5-meter unpumped EDF is used as a self-induced FBG filter, which dynamically tracks the wavelength tuning of a fiber Fabry-Perot tunable filter (FFP-TF). Theoretical modeling brought forth valid SLM condition and then a series of experiments proved SLM laser operation. The laser can be wavelength-swept over the entire C-band (1520nm-1570nm) window with linewidth less than 0.7 kHz. The optimum sweeping frequency in order to achieve the best output power stability was experimentally found to be 20 Hz with swept-induced high frequency power fluctuation of only 0.1%.

2. Experimental setup

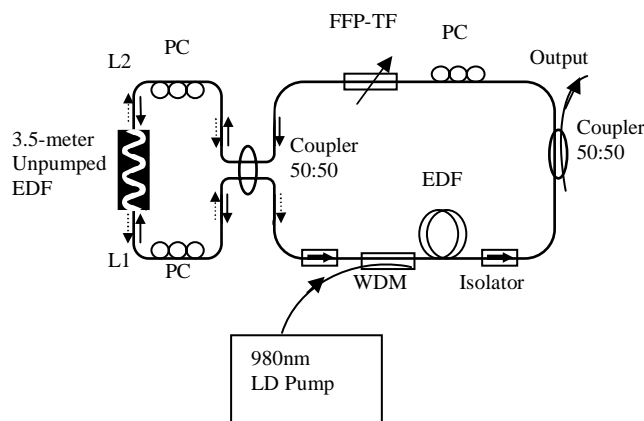


Fig. 1. Schematic layout of the tunable SLM EDF ring laser

A schematic layout of the tunable SLM EDF ring laser is shown in Fig. 1. The erbium doped fiber amplifier (EDFA) section consists of a 15-meter EDF as the gain medium, pumped by a 980nm laser diode (LD) through a 1550nm / 980nm wavelength division multiplexer (WDM) coupler. Two optical isolators are placed in the input and output of EDFA to ensure the unidirectional lasing operation and to prevent any feedback that could cause instabilities in the cavity. An electrically driven intra-cavity FFP-TF with a bandwidth of 25GHz provides a coarse first-stage wavelength selection. Using a 3-dB fiber coupler, a Sagnac loop is formed and an unpumped 3.5-meter EDF is inserted into the loop. The unpumped EDF functions as a saturable absorber and forms a self-induced FBG with an ultra-narrow bandwidth and dynamically tracks the wavelength of the FFP-TF. Theoretical modeling in Section 3 shows that this structure can provide a fine second-stage filtering which ensures SLM lasing. Polarization controllers (PC) are inserted in both the main fiber cavity and the Sagnac loop to control the cavity birefringence. A 3-dB coupler was used as an output coupler of the laser. The total ring cavity was measured to be approximately 23m, which corresponds to a longitudinal mode space of 9 MHz. All components were fusion spliced to reduce back reflection and high transmission between components.

3. Modeling for mode selecting by Sagnac loop incorporated with unpumped EDF

As shown in Fig. 1, the incident light to the Sagnac loop shown as a solid arrow on the left side of the loop is splitted into two identical waves by the 50:50 coupler forming the Sagnac loop. These two waves subsequently counter-propagate in the unpumped EDF. A standing wave (white wave line inside the EDF) is thus formed [10], and the spatial period of light intensity distribution can be easily determined to be $\lambda/2n_{\text{eff}}$ from the standing wave theory, where λ is the central wavelength and n_{eff} is the effective refraction index of the EDF. Consider the two-level system consists of energy levels $^4I_{15/2}$ and $^4I_{13/2}$ of erbium ion, where saturable absorption coefficient can be written as [11]:

$$\alpha(z) = \frac{\alpha_0}{1 + I(z)/I_{\text{sat}}} \quad (1)$$

where I_{sat} is the saturation intensity. As the result of the spatial periodical distribution of the light intensity $I(z)$, the absorption coefficient $\alpha(z)$ also varies periodically. This results in periodical spatial variation of refraction index, given by the Kramers-Kronig relation [12]:

$$\Delta n(z, \omega) = \frac{c}{\pi} P.V. \int_{\omega_1}^{\omega_2} \frac{\Delta \alpha(z, \omega')}{(\omega')^2 - \omega^2} d\omega' \quad (2)$$

where P. V. is the principal value of the integral derived over the frequency range $\omega_1 < \omega < \omega_2$. For this laser system, we used low-doped EDF (doping concentration $\rho < 10^{19} \text{ Er}^{3+}/\text{cm}^3$) and the maximum intra-cavity power was limited under 20 mW. Therefore we can easily deduce induced refraction index change which is estimated to be $\Delta n < 3 \times 10^{-7}$ [13]. Therefore, a weakly coupled FBG with a period of $\Lambda = \lambda/2n_{\text{eff}}$ is induced by the incident light itself inside the unpumped EDF. The reflected light is then combined and transmitted through the coupler (dotted arrows in Fig. 1). The transmission of the Sagnac loop incorporated with an FBG can be then written as [14]:

$$T = \frac{[(1 - 2K)\sqrt{1 - \delta^2 / \kappa^2} + 2\sqrt{K(1 - K)} \sinh(\sqrt{\kappa^2 - \delta^2} L_g) \cos(\beta \Delta L)]^2}{\cosh^2(\sqrt{\kappa^2 - \delta^2} L_g) - \delta^2 / \kappa^2} \quad (3)$$

where β is the mode propagation constant, $\delta = \beta - \pi/\lambda$ is the detuning, κ is the coupling coefficient of the grating, L_g is the grating length, K is coupling coefficient of the coupler,

$\Delta L=L_1-L_2$ is the difference of the fiber lengths shown in Fig. 1. For $K=0.5$ and $\Delta L=0$, we get the same transmission as a typical FBG:

$$T = \frac{\sinh^2(\sqrt{\kappa^2 - \delta^2} L_g)}{\cosh^2(\sqrt{\kappa^2 - \delta^2} L_g) - \delta^2 / \kappa^2} \quad (4)$$

The full-width-half maximum (FWHM) bandwidth of the induced FBG can be written as [15]:

$$\Delta f = \frac{c}{\lambda} \kappa \sqrt{\left(\frac{\Delta n}{2n_{eff}}\right)^2 + \left(\frac{1}{N}\right)^2} \quad (5)$$

where $N=L_g/\Lambda$ is the total number of grating periods, and λ is the central wavelength at which maximum reflectivity occurs. The coupling coefficient of the induced grating κ can be estimated from Δn as [16]:

$$\kappa = \frac{2\Delta n}{n_{eff}\lambda} \quad (6)$$

If we take the values: $\lambda=1540\text{nm}$, $L_g=3.5\text{m}$, $n_{eff}=1.45$ and $\Delta n < 3 \times 10^{-7}$, from Eq. (5) and Eq. (6) we can estimate the FWHM of Sagnac loop with self-induced FBG as $\Delta f < 5.6\text{ MHz}$. Considering the 9 MHz longitudinal mode space of the fiber ring cavity, the SLM operation condition is well satisfied.

4. Experimental results and discussion

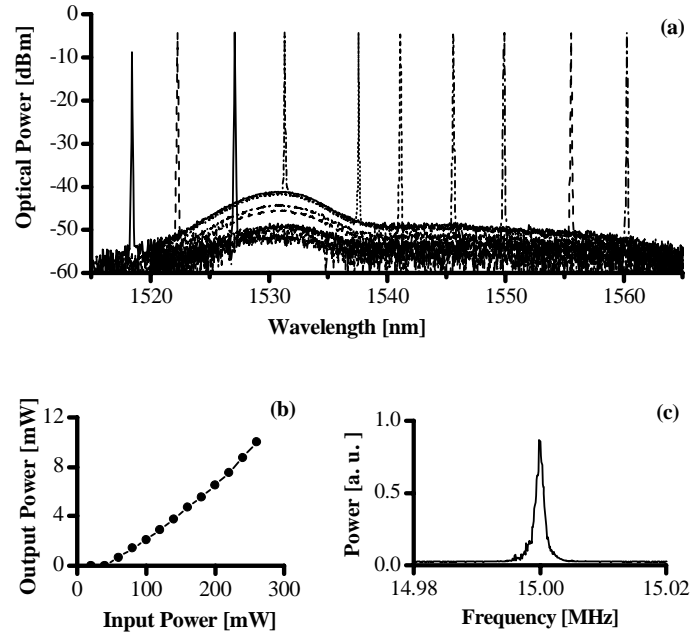


Fig. 2. (a) OSA measured output spectrum of the laser under the pump power of 100mW. (b) Measured output laser power as a function of the 980nm LD input pump power. (c) RF spectrum of delayed self-heterodyne signal

By changing the voltage applied to the FFP-TF, while maintaining a constant pump power of 100mW we measured the output spectrum of the laser using an optical spectrum analyzer (OSA), as shown as Fig. 2(a). The laser tuning range achieved was more than 45nm, the full width of the C band (1520nm-1570nm), and the power variation over the entire tuning range was less than one dB if we neglect the wavelength below 1520 nm. Figure 2(b) shows the measured output laser power at 1550 nm as a function of the 980nm LD input pump power. The laser threshold was 45mW and the conversion efficiency was 5%. The low conversion efficiency is mainly due to the high absorption loss in the Sagnac loop. Figure 2(c) shows a delayed self-heterodyne RF spectrum of the laser output which was used to measuring the spectral linewidth of the laser output. A 20-km-long single mode fiber was used as the delay line and an acoustic optical modulator operating at 15MHz was used in one arm of the delayed self-heterodyne set-up to shift the beat frequency away from DC. The RF spectral was fitted and the spectral linewidth of the laser was deduced to be less than 0.7 kHz.

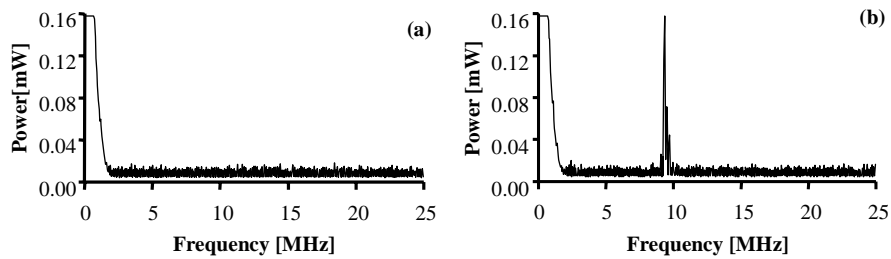


Fig. 3. Noise spectrum of output laser (a) with 3.5-meter EDF and (b) with 0.3-meter EDF.

To verify the SLM operation condition of our laser, we measured the RF spectrum of the laser output by a high speed photodetector and RF spectrum analyzer, as show in Fig. 3(a). As expected there are no beat and high frequency RF signal caused by adjacent modes since the laser operates in SLM. As a comparison, we replaced the 3-meter EDF with a 0.3-meter one, which according to Eq. (5) gave a much larger FWHM of $\Delta f < 65$ MHz. In this case the SLM status is not guaranteed and as a result we can see strong beat signal around 9 MHz in Fig. 3(b).

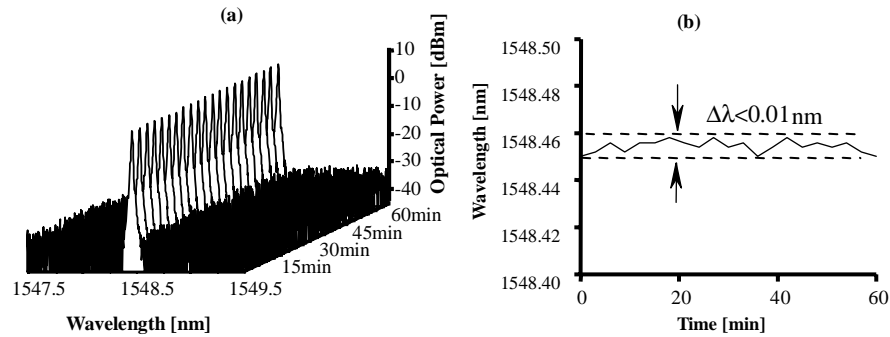


Fig. 4. (a) Measured output spectrum at fixed wavelength of 1548.45nm every 3 minutes for 60 minutes. (b) Fluctuation of wavelength during 60 minutes.

Figure 4(a) shows the measured output spectrum at fixed wavelength of 1548.45nm for 60 minutes under the pump power of 200mW. The output power is 8.1 dBm and the signal-to-noise ratio is ~50dB. No significant variation in the spectrum shape is observed from

measurements at different time points. The wavelength fluctuation is less than 0.01nm which is due to thermal drift, shown as Fig. 4(b).

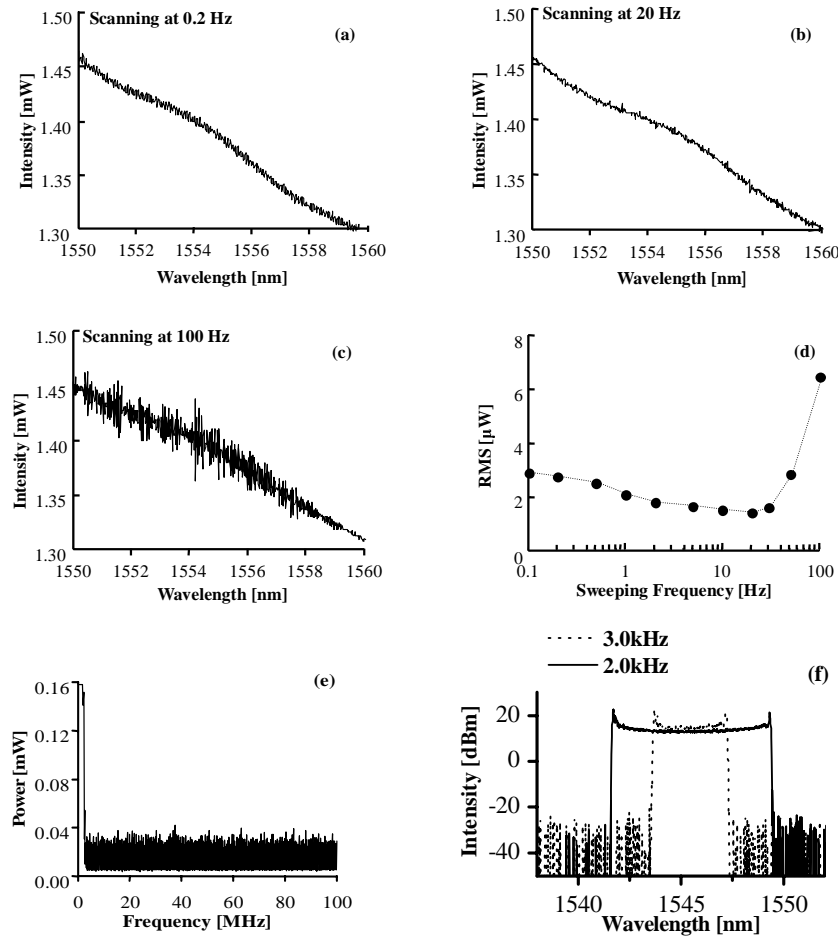


Fig. 5. (a)~(c) Output power intensity as function of wavelength at sweeping frequency of 0.2Hz, 20 Hz and 100Hz respectively. (d) RMS of output power as a function of sweeping frequency. (e) Noise spectrum of output laser at sweeping frequency of 20 Hz. (f) Peak-hold (persistence mode) spectra of the lasing modes when triangle waveforms are applied to the FFP-TF, with frequencies of 2.0 kHz (solid line) and 3.0 kHz (dot line) respectively.

By applying RF triangle signal from a function generator, the central wavelength of the FFP-TF can be continuously swept. Figure 5(a) ~ (c) are the measured output performance at different sweeping frequency of the FFP-TF over the spectrum range of 1550nm~1560nm. From Fig. 5(d), in respect to output power stability, we can find the optimum sweeping frequency to be around 20 Hz, which gives the minimum root-mean-square (RMS) of the output power of 1.5 μ W. At the optimum frequency, the laser out put is very stable with power fluctuation (the high frequency variation due to the wavelength sweeping) of only 0.1 %. In addition, we have measured the noise spectrum over 0~ 100 MHz of the output when the laser was sweeping at 20 Hz which is shown in Fig. 5(e). As can be seen from the spectrum, there are no beat and high frequency RF components which proves that the laser maintains its SLM

operation even operating in the swept mode. The above features together with solid wavelength stability and narrow linewidth enable the laser a number of spectroscopic and sensing applications, especially in ultra-high-resolution spectroscopy and sensory of trace gases.

A 23 dBm EDFA was used to amplify the laser output and the swept laser spectrum was measured under peak-hold mode of OSA, as shown in Fig. 5(f). At the frequency of 2.0 kHz, the power fluctuation is only about 1dBm and a very stable output spectrum is obtained.

However, the laser sweeping frequency and range is limited by the maximum frequency response of the FFP-TF and the total laser cavity length, which is just a little above 3 kHz. The main focus of our work was to achieve stable single-longitudinal-mode wavelength sweep operation but not to achieve high frequency operation. Nevertheless as shown in Fig. 5(f), with the same triangle waveform, when the frequency is changed from 2.0 kHz (solid line) to 3.0 kHz (dot line), the laser is decreased in sweeping range but still with stable spectrum. Therefore it is possible to increase the sweeping range and frequency by using a higher speed and more stable FFP-TF, which can reach the frequency of a few tens of kHz [17], and also a shorter gain length in the cavity can improve the laser sweeping performance [18].

Compared to other works which also used unpumped EDF as a saturable absorber, but with FBGs as wavelength selector [4,10], our laser scheme is simpler to build, easier to control for sweeping operation, less vulnerable to temperature perturbation than FBGs and has much narrower sub-kHz linewidth.

5. Summary

We designed and demonstrated a wavelength-swept EDF ring laser that operates in stable SLM. A Sagnac loop with a 3.5-meter unpumped EDF was used as a self-induced FBG filter, which dynamically tracks the wavelength of a fiber Fabry-Perot tunable filter (FFP-TF). Theoretical modeling was used to validate SLM condition and this was proved by a series of experiments. The laser is continuously tunable over 45nm over the entire C-band (1520nm-1570nm) with linewidth less than 0.7 kHz. The optimum sweeping frequency in order to achieve the best power stability was experimentally found to be ~20 Hz with power fluctuation of only 0.1%.